

Dear Solid Earth Editor,

Please find below the point-by-point responses to the reviewer comments, as well as the original Word file annotated with changes tracked so that you can easily see the changes  
5 that were made in response to the reviewer comments.

We believe that we have taken care of all of the reviewer comments, and hope that you will find the manuscript now acceptable for publication in Solid Earth.

10 We look forward to hearing from you soon.

Sincerely,

David A. Ferrill, 5 April 2020

15

---

**Author response to Tiago Alves' Interactive comment on "Resolved stress analysis, failure mode, and fault-controlled fluid conduits in low-permeability strata" by David A. Ferrill et al.**

**David A. Ferrill, Kevin J. Smart, Alan P. Morris (Authors)**

20

**Comment** – “Dear authors, I liked reading your paper, particularly after acknowledging that the analysis in this work is similar to that we have developed at Cardiff since we first contacted SWRI in 2013 - and collaborated with this latter institute. With this in mind, se-2020-17 is an excellent addition to what has been an attempt at characterizing fault-related fluid flow using high-quality seismic data. I was very  
25 pleased with having a field analogue of what we see on seismic.”

**Author's Response** – Thank you for the positive feedback!

**Author's Change in Manuscript** – Revised manuscript will enhance comparison to published examples and observations based on high-quality seismic data.

30 **Comment** – I think this paper needs a moderate revision, and I appended an annotated .pdf to this review.

**Author's Response** – Accept.

**Author's Change in Manuscript** – Manuscript revision will address comments in annotated .pdf provided by reviewer.

35 **Comment** – Title - is the analysis in this work only valid for low-permeability data? I feel the analysis is broader than the title suggests.

**Author's Response** – Accept, good point.

**Author's Change in Manuscript** – Title is being shortened by removal of “in low-permeability strata” as suggested by reviewer.

40

**Comment** – 1-Very old references are used at the start of the paper. Why such broader references when the paper is very much about fault slip and associated tendency to leak?

**Author's Response** – Accept.

**Author's Change in Manuscript** – Additional more recent relevant references are being added in the  
45 revision, as suggested by the reviewer.

**Comment** – 2 and 3-Seismic-based analyses have been undertaken by N. Ward et al. (2016). Tectonophysics and Roelofse et al. (2019) in basins posed for CO2 capture and storage. I would suggest the authors to indicate that low-permeability intervals have been characterized in detail using high-quality  
50 seismic data and borehole information.

**Author's Response** – Accept.

**Author's Change in Manuscript** – Additional relevant references for CO2 sequestration and examples characterized using seismic and borehole information are being included in the revision, as suggested by the reviewer.

55

**Comment** – 4-Case studies are missing at the end of Page 1.

**Author's Response** – Accept.

**Author's Change in Manuscript** – Case studies from the literature are being added in support of this, as suggested by reviewer.

60

**Comment** – 5 & 6 - This part hints at the problem of scale in fault segment interaction. At what scale this interaction occurs? Could you kindly complete this introduction with the comments and ideas in Tao and Alves (2017) Reply letter and Tao and Alves (2019). Tectonophysics? These are important papers that review the importance of understanding fault segment length at several scales of analysis - without under-  
65 interpreting data - as fluid flow will be controlled by elusive roughness, pull aparts and local refraction features in faults. It is reassuring to see this paper (se-2020-17) confirm the aspects in Tao and Alves (2017; 2019).

**Author's Response** – Accept.

**Author's Change in Manuscript** – Revised manuscript will expand on this and include the relevant  
70 suggested references.

**Comment** – 7-Once again, examples exist of similar approaches in Ward et al. (2016) and Roelofse et al. (2019). Mattos et al. (2016; 2018) are also interesting papers from Cardiff.

**Author's Response** – Accept.

75 **Author's Change in Manuscript** – Revised manuscript will expand on this and include the relevant suggested references.

**Comment** – 8-low permeability, rather than 'impermeable' strata. There is no such thing as impermeable strata.

80 **Author's Response** – Accept.

**Author's Change in Manuscript** – Revised text will use adjusted language as suggested.

**Comment** – 9-Total/maximum lengths of faults need to be stressed at the start of the paragraph. Which stratigraphic section? Detail needed.

85 **Author's Response** – Accept.

**Author's Change in Manuscript** – Requested detail will be included in the revised manuscript.

**Comment** – 10 (page 8) - The 'scale problem' arises once again. Do the fault segments obey the rules in Tao and Alves (2019) that we need to collect T/Z data at a minimum spacing of 5% of a fault zone length to identify the presence of discrete segments; otherwise faults will resemble large constant-length structures? I am not asking for the inclusion of T/Z data in your paper, but it would be good to understand if the 5% rule is clearly recognized in the field - note: some longer faults require T/Z measurements at 3% of the length of a fault zone so that one can identify discrete segments. I think 2-3 paragraphs confirming how the segments are identified in se-2020-17 is very important in this page 8.

95 **Author's Response** – Accept.

**Author's Change in Manuscript** – The revised manuscript will discuss the identification of discrete segments as suggested.

**Comment** – 11-Add examples with work undertaken by the Cardiff group using seismic data. The stress tensors are rather similar to some of our work.

**Author's Response** – Accept.

**Author's Change in Manuscript** – Revised manuscript will make reference to this other published work as suggested and appropriate.

105 **Comment** – 12-Segment scale needs to be referred to once again. Do they obey the field observations, which are seemingly based on the recognition of linkage points and inflexion/trend changes in discrete fault segments? (see Tao and Alves, 2017 Reply).

**Author's Response** – Accept.

**Author's Change in Manuscript** – Segment scale will be addressed in the revised manuscript

110

**Comment** – In essence, I overly enjoyed to read this work. The comments above will broaden the scope of this paper - particular those referring to the scale of fault and joint segments in the field and the way(s) they are recognized.

**Author's Response** – Accept – thank you!

115 **Author's Change in Manuscript** – Revisions to the manuscript will broaden the scope as recommended.

**Comment** – Please also note the supplement to this comment:

<https://www.solid-earth-discuss.net/se-2020-17/se-2020-17-RC1-supplement.pdf>

**Author's Response** – Accept.

120 **Author's Change in Manuscript** – The marked up manuscript supplement is being consulted in addressing the reviewers comments.

---

**Author response to Fabio Trippetta's Interactive comment on "Resolved stress analysis, failure mode, and fault-controlled fluid conduits in low-permeability strata" by David A. Ferrill et al.**

125 **David A. Ferrill, Kevin J. Smart, Alan P. Morris (Authors)**

**Comment** – The paper "Resolved stress analysis, failure mode, and fault-controlled fluid conduits in low-permeability strata" by Ferrill et al., is well organized and deals with the very interesting topic of mechanical models (generally speaking) where the authors are very expert. I really enjoyed reading it.

130 **Author's Response** – **Accept** – Thank you for the positive feedback!

**Author's Change in Manuscript** – No change needed to address this comment.

**Comment** – The paper follows some previous works extending theoretical models to real faults deeply studied previously by the same authors. In light of this, the boundary conditions of the applied mechanical model should be very well explained and constrained, in my opinion, in order to give to the reader all the instruments to completely understand the meaning of the results. This is the part of the paper that I think should be improved.

135 **Author's Response** – Accept.

**Author's Change in Manuscript** – Additional detail to address stress and geomechanical assumptions and interpretations will be included in the revised manuscript.

140

**Comment** – In particular it is not clear to me for example what are the constraints for the hypothesized pore pressure, being this quite high ( $\lambda$  over 0.7). The same for the mechanical properties of the involved lithologies proposed in Figure 6. No indication is reported along the paper about the source for the adopted mechanical data such as for example cohesion and coefficient of friction.

145 **Author's Response – Accept.**

**Author's Change in Manuscript** – Additional explanation of pore pressure, stress, and geomechanical assumptions and interpretations will be included in the revised manuscript.

**Comment** – Keeping the focus on Fig. 6 the proposed model is not clear to me. Since no build-up processes for fluid pressure are invoked along the text, if I well understand, rocks will fail in the initial stage, for a decrease of the  $\sigma_3$  being the system in an extensional regime. This bring mudrock to break first as showed in the model. Thus, at this time, a decrease in pore pressure is expected since, generally speaking, a rupture is related to an increase in permeability/porosity that lead to a decrease in pore pressure. However, following the model, a continuous process of build up for fluid pressure should be present in the system in order to overcome the  $\sigma_3$  and bring to hydraulic fractures on chalk. So I am wondering how can we reach the condition for high overpressure on chalk if a rupture already occurred on mudrock. That said, should we assume different boundary conditions for mudrock and chinks and reconsider figure 3?

**Author's Response** – Because of different mechanical properties of mudrock and chalk, response to loading conditions produces significantly different pre-failure responses in mudrock versus chalk, and therefore different effective stress conditions from one mechanical layer to the next through the section. We are not specifically interpreting whether mudrock or chalk failed first. However, the repeated occurrence of refracted fault propagation through the section, contrasting mechanical properties of chalk and mudrock, and absence of widespread hybrid failure in chalk beds or shear failure in mudrock that is unassociated with larger multi-bed faults, suggests distinctly different effective stress conditions in mudrock and chalk shown in Fig. 6b likely coexisted in adjacent beds during fault propagation.

**Author's Change in Manuscript** – Text will be modified in the manuscript revision to further clarify this point.

165

**Comment** – In conclusion I think that this very interesting paper deserves some more rigorous constraints for the applied mechanical model. Moreover, a more comprehensive discussion on the model implication and on its evolution over time and space will strongly improve the paper together with a comparison with results from other authors (see line to line comments).

**Author's Response** – Accept.

170 **Author's Change in Manuscript** – Thank you for the positive feedback. Additional discussion and references will be included in the revised manuscript, as suggested by reviewer.

**Comment** – Some line to line notes are on the pdf attached file. Hope this helps, Fabio Trippetta

Please also note the supplement to this comment: <https://www.solid-earth-discuss.net/se-2020-17/se-2020-17-RC2-supplement.pdf>

175

**Author's Response** – Accept – thank you.

**Author's Change in Manuscript** – The marked-up manuscript supplement is being consulted in revising the manuscript.

+++++

# Resolved stress analysis, failure mode, and fault-controlled fluid conduits in low-permeability strata

David A. Ferrill<sup>1</sup>, Kevin J. Smart<sup>1</sup>, Alan P. Morris<sup>1</sup>

<sup>1</sup> Southwest Research Institute, 6220 Culebra Road, San Antonio, Texas 78238-5166, USA

185 *Correspondence to:* David A. Ferrill (dferrill@swri.org)

**Abstract.** Failure behaviours can strongly influence deformation-related changes in volume, which ~~is~~ are critical in the formation of fault and fracture porosity and conduit development in low permeability rocks. This paper explores the failure modes and deformation behaviour of faults within the mechanically layered Eagle Ford Formation, an ultra-low permeability self-sourced oil and gas reservoir and aquitard exposed in natural outcrop in southwest Texas, U.S.A. Particular emphasis is placed on analysis of the relationship between slip versus opening along fault segments, and the associated variation in dilation tendency versus slip tendency. Results show that the failure mode and deformation behaviour (dilation versus slip) relate in predictable ways to the mechanical stratigraphy, stress field, and specifically the dilation tendency and slip tendency. We conclude that dilation tendency versus slip tendency patterns on faults and other fractures can be analysed using detailed orientation or structural geometry data and stress information, and employed predictively to interpret deformation modes and infer volume change and fluid conduit versus barrier behaviour of structures.

## 1 Introduction

Faults and fractures often serve as conduits for fluid in low permeability rock (Barton et al., 1995; Caine et al., 1996; Zoback et al., 1996; Evans et al., 1997; Sibson and Scott, 1998; Ferrill and Morris, 2003; Faulkner et al., 2010; [Alves and Elliott, 2014](#); [Mattos et al., 2016](#); [Mattos and Alves, 2018](#); [Roelofse et al., 2020](#)), including self-sourced oil and gas reservoirs (Ferrill et al., 2014a, 2014b, 2020; Gale et al., 2014), or CO<sub>2</sub> reservoirs ([Trippetta et al., 2013](#); [Ward et al., 2016](#); [Miocic et al., 2020](#)), and reservoir cap-rock seals (e.g., Petrie et al., 2014; [Roelofse et al., 2019](#)). Permeability behaviour – flow pathway versus seal – can be directly related to the deformation modes along a fault, fracture, or fracture network (Carlsson and Olsson, 1979; Sibson, 1996, 1998, 2000, 2003; [Trippetta et al., 2017](#); Ferrill et al., 2019a). In any applied stress field, multiple deformation features may form coevally, with failure initiation occurring at varying orientations and in different failure modes (e.g., Hancock, 1985; Lee et al., 1997; Lee and Wiltschko, 2000; Ferrill & Morris, 2003; Schöpfer et al., 2006; Busetti et al., 2014; Maher, 2014; Smart et al., 2014; Douma et al., 2019; Boersma et al., 2020). Deformation behaviour, and in particular positive or negative dilation versus shear, is closely related to the orientation of the failure plane or zone with respect to the stress field at the time of deformation (e.g., Ramsey and Chester, 2004; Ferrill et al., 2017b). Recent work has shown that failure or reactivation

mode along faults can be directly related to the dilation tendency versus slip tendency on the fault in the stress field at the time  
210 of deformation (**Fig. 1**; Ferrill et al., 2012, 2017a, 2019b; [Ward et al., 2016](#); [Meng et al., 2020](#), [Miocic et al., 2020](#); [Roelofse  
et al., 2020](#)).

In this paper, we explore the variability of resolved stress patterns along well-exposed and preserved, small displacement  
normal faults in the Eagle Ford Formation, and the relationship between dilation tendency, slip tendency, and deformation  
behaviour (failure mode) at various positions along faults following the approach presented by Ferrill et al. (2019a). The faults  
215 at the study site exhibit many segments that have measureable shear displacement and slickenlines, and other segments that  
have dilated and are partially or fully mineralized with calcite from the paleo-movement of aqueous fluids. Observations show  
that failure modes along individual faults can vary dramatically over ~~short~~ distances (~~of a few cm~~), governed by the lithologic  
changes and fault segment interaction. Shear versus dilational behaviour relates directly to the mechanical stratigraphy and  
the orientation of the failure zone within the stress field at the time of deformation (Ferrill and Morris, 2003). This study  
220 provides a clear example of how faults can serve as fluid conduits in mechanically layered low permeability strata.  
[Furthermore, this work supports conclusions from seismic-scale observations that fault oversimplification misrepresents fault  
geometries and related damage zones, which translates to unreliable estimation of fault sealing behaviour \(Ze and Alves, 2019\).](#)  
~~Furthermore,~~ ~~†~~The use of dilation tendency versus slip tendency patterns shows significant potential for predicting failure or  
reactivation mode on faults or fractures, and the related conduit versus seal behaviour of those structures, applicable to detailed  
225 faults and fractures mapped or imaged in the subsurface.

## 1 Background

The Cretaceous Eagle Ford Formation has become an important self-sourced unconventional oil and gas reservoir in south  
Texas, U.S.A. (Robinson, 1997; Martin et al., 2011; Cusack et al., 2010; Bodziak et al., 2014; Breyer et al., 2016), and an  
organic rich source rock for migrated oil produced out of other formations including the directly overlying Austin Chalk and  
230 underlying Buda Limestone (Edman and Pitman, 2010; Zumberge et al., 2016; Kornacki, 2018). In up-dip regions closer to  
the Eagle Ford outcrop belt along the Balcones fault zone, the Eagle Ford is an aquitard that forms a barrier to communication

between aquifers including the overlying Austin Chalk, underlying Buda Limestone, and the deeper Edwards Aquifer (Livingston et al., 1936; Maclay and Small, 1983; Maclay, 1989; Ferrill et al., 2004, 2019b).

Analyses of the Eagle Ford oil and gas reservoir have shown the formation to have ultra-low permeabilities (50-1500 nanodarcies; Denney, 2012). This helps to explain the retention of self-sourced oil and gas in the formation, as well as the role of the formation as a barrier to fluid movement. Recent outcrop studies, however, have shown that small-displacement faults – displacements of cm’s to m’s – within organic rich Eagle Ford Formation and overlying Austin Chalk that never reached oil window conditions necessary for hydrocarbon maturation are locally mineralized with calcite that contains fluorescent liquid hydrocarbon inclusions (Ferrill et al., 2014a, 2017a, 2020). Calcite cements in fault zone veins within the Eagle Ford Formation and Austin Chalk show crack-seal textures indicative of numerous incremental slip events, providing clear indication of porosity generation and water movement from which the calcite precipitated (Ferrill et al., 2014a, 2017a, 2020). Migrated-oil inclusions in the calcite indicate longer distance up-dip travel of oil (likely tens of km) from areas where source rock strata reached oil generation conditions (Ferrill et al., 2020). Analyses of homogenization temperatures for two-phase (liquid-vapour) inclusions indicate fluid trapping at 1.4 to 2.9 km depths, and possibly as deep as 4.2 km (Ferrill et al., 2014a, 2017a, 2020). These trapping depth estimates indicate that the faults analysed here formed and remained active at these depths, and are not near-surface phenomena. For comparison, these depths of normal fault formation and fluid movement are analogous to fault controlled fluid flow based on 3D seismic interpretation in the Barents Sea (Mattos et al., 2016), North Sea (Alves and Elliot, 2014; Ward et al., 2016), and the Gulf of Mexico (Roelofse et a., 2020).

Refracted fault shapes and associated localization of dilation and cementation along these faults indicate the intricate interplay between mechanical stratigraphy and failure modes, and bed-to-bed switching in failure and reactivation behaviour that led to formation of conduits for fluid flow through the otherwise ~~nearly impermeable~~ very low permeability Eagle Ford Formation. Better understanding of the structural processes that influence formation of fault controlled fluid conduits is needed to evaluate migration and accumulation of hydrocarbons, as well as integrity of very low permeability sealing strata. Furthermore, this improved understanding could also aid interpretation of failure modes and fracture geometries produced by hydraulic fracturing in the Eagle Ford Formation and other mechanically layered unconventional reservoirs.

### 3 Methods

### 3.1 Fault segment characterization

Analyses in this paper focus on three faults in the Eagle Ford Formation exposed in bluffs along Sycamore Creek in southwest

260 Texas. The three faults, in order of increasing displacement, are the (i) Textbook fault (max. throw in exposure = 10 cm; exposed height measured tip-to-tip = 7.2 m; Fig. 2), (ii) Spanish Goat fault (max. throw in exposure = 35 cm; exposed height from base of exposure to upper tip = 6 m), and (iii) Big Indigo fault (max. throw in exposure = 6 m; cuts entire 30 m height of exposure). These three faults are only exposed in the bluff, and cannot be mapped beyond the width of the cliff exposure.

These faults were previously discussed and analysed by Ferrill et al. (2017a) and were selected from the larger population of

265 faults at Sycamore Bluffs for detailed analysis because they (i) represent the spectrum of displacements on faults in the exposure, (ii) are in close proximity to each other, and (iii) represent faulting in the mudrock and chalk dominated pelagic reservoir section of the Eagle Ford Formation (Lehrmann et al., 2019). With respect to the measured section in Ferrill et al.

(2017; their figure 3), measurements from the Textbook fault are from stratigraphic heights 1.25 m to 7.8 m, measurements from Spanish Goat fault are stratigraphic heights 4.6 m to 8.9 m, and measurements from the Big Indigo fault are from stratigraphic heights 5.35 m to 7.1 m. cut approximately the same portion of the stratigraphic section. ~~The three faults, in~~

270 ~~order of increasing displacement, are the (i) Textbook fault (max. throw in exposure = 10 cm; Fig. 2), (ii) Spanish Goat fault (max. throw in exposure = 35 cm), and (iii) Big Indigo fault (max. throw in exposure = 6 m).~~ Fault segments through different

lithologic beds were mapped in the field directly onto digital photographs, and strike, dip, and rake (where slickenlines were visible) were measured using Brunton compass. Displacements were measured using metric measuring tape for the smaller

275 displacement faults (i.e., Textbook fault, Spanish Goat fault, and NW segment of Big Indigo fault). The displacement of several meters and irregularity of the outcrop surface precluded direct field measurement of displacement on the main strand of the Big Indigo fault. Consequently, we surveyed the main trace of the Big Indigo fault using a spatial scanning system

(Trimble VX™ Spatial Station) to measure the three-dimensional positions of offset marker beds at their hanging wall and footwall cutoffs, and from those data extracted displacements. The three faults analysed here exhibit significant changes in

280 dip of the failure surfaces, and exhibit variation in deformation behaviour, including slickenlined slip surfaces and dilational segments that are partially or completely calcite-filled (Fig. 2).

### 3.2 Stress field interpretation

285 Stress inversion was performed using orientations of fault slip surfaces and displacement measurements from measured slip  
surfaces along the Textbook, Spanish Goat, and Big Indigo faults. The inversion was performed using the technique of  
McFarland et al. (2012) as implemented in 3DStress v. 5.1 (Morris et al., 2016). We adjusted the stress tensor solution slightly  
to align the intermediate principal compressive stress ( $\sigma_2$ ) orientation with the minimum eigenvector from the fault population  
because we expect  $\sigma_2$  to be parallel to the intersection line direction for a conjugate normal fault population (Anderson, 1951;  
Thompson, 2015).

290

### 3.3 Dilation tendency and slip tendency analysis

Dilation tendency and slip tendency of a deformation feature or other fabric element are controlled by the orientations and relative magnitudes of the principal stresses in the imposed stress state. Dilation tendency ( $T_d$ ) was defined by Ferrill et al. (1999) by the following Eq. (1):

$$295 \quad T_d = \frac{(\sigma_1 - \sigma_n)}{(\sigma_1 - \sigma_3)}, \quad (1)$$

where  $\sigma_n$  = resolved normal stress,  $\sigma_1$  = maximum principal compressive stress, and  $\sigma_3$  = minimum principal compressive stress. Slip tendency ( $T_s$ ), was defined by Morris et al. (1996) by the following Eq. (2):

$$T_s = \frac{\tau}{\sigma_n}, \quad (2)$$

300 where  $\tau$  = resolved shear stress. Dilation tendency and slip tendency analyses were performed in 3DStress, using the derived  
stress tensor and the measured orientations of the deformation features.

## 4 Results

### 4.1 Fault segment characterization

305 Data were collected ~~from 141~~representing 142 measurement positions along the three faults, tracking refracted faults through  
multiple lithologic layers. Orientation measurements were made from matching failure surfaces along both the hanging wall  
and footwall cutoffs for each measured bed cut by the fault (Textbook fault, n = 28; Spanish Goat fault, n = 23; Big Indigo  
fault, n = 20). The three faults represent progressive stages of increasing fault displacement and fault zone development. The  
faults have refracted fault profiles with numerous dip changes (e.g., **Fig. 2a**). These refracted profiles are represented not only

by changes in dip, but also by changes in deformation behaviour, ranging from thin slip surfaces exhibiting slickenlines to  
310 thick calcite veins with crack-seal textures representing significant dilation and numerous dilational slip events. Some  
dilational fault segments are only partially filled with calcite cement and exhibit euhedral crystal terminations indicative of  
crystal growth into open voids (**Fig. 2b**). Most of the dilational fault segments, however, are completely filled with calcite  
(e.g., **Fig. 2c**), as described in Ferrill et al. (2017a). Calcite-cemented fault segments tend to have steep to vertical dips ( $\geq 75^\circ$ ).  
In contrast, gently to moderately dipping fault segments ( $< 30\text{--}75^\circ$ ) typically are marked with slickenlines, lack calcite cement,  
315 and reflect little or no positive dilation suggestive of shear or compactive-shear deformation. Measurement spacing (as a  
function of height of the survey portion of the fault) represents (i) 3.6% of the analyzed profile of the Textbook fault, (ii) 4.3%  
of the analyzed portion of the Spanish Goat fault (partial height of the fault), and (iii) 9.1 % of the analysed height of the Big  
Indigo fault main trace (partial height of fault). A recent study by Ze and Alves (2019) mapped faults using 3D seismic  
reflection data and explored throw versus distance and throw versus depth profiles, and associated slip tendency and leakage  
320 factor analyses. Among Ze and Alves' (2019) conclusions were recommendations that sampling be performed at spacing of  
<5% for faults < 3500 m long, and <3% for faults >3500 m – our —our results would generally support these recommendations.

## 4.2 Stress field interpretation

The interpreted stress tensor used in the dilation tendency and slip tendency analyses is defined by the following relative  
325 magnitudes and orientations of the principal stresses as follows (**Fig. 3**):  $\sigma_1 = 1.00$ , azimuth  $170^\circ$ , plunge  $71^\circ$ ;  $\sigma_2 = 0.65$ ,  
azimuth  $019^\circ$ , plunge  $17^\circ$ ;  $\sigma_3 = 0.30$ , azimuth  $286^\circ$ , plunge  $9^\circ$ . As noted earlier, we slightly adjusted the orientation of  $\sigma_2$   
from the initial stress inversion to align with the minimum eigenvector from the fault slip surface population (i.e., orientation  
changed from  $017^\circ/25^\circ$  to  $019^\circ/17^\circ$ ). If we assume approximately 2 km of overburden, consistent with depths of 1.4 to 2.9  
km (possibly as deep as 4.2 km) estimated from fluid inclusion analysis of veins from these and nearby faults (Ferrill et al.,  
330 2014a, 2017a, 2020); —with an average density of 2500 kg/m<sup>3</sup>, consistent with the sedimentary overburden in the region; —and  
adjust for overpressured pore pressure conditions (0.018 MPa/m), consistent with observations of overpressured in the Eagle  
Ford reservoir under production in south Texas. T—the three principal effective stress ( $\sigma'$ ) magnitudes (adjusted for pore fluid  
pressure; cf. Ward et al., 2016) at the time of failure in mudrock are estimated to be (i)  $\sigma'_1 = \sim 15$  MPa, (ii)  $\sigma'_2 = \sim 10$  MPa;

and (iii)  $\sigma'_3 = \sim 5$  MPa. As noted earlier, dilation tendency and slip tendency are controlled by the orientations and relative magnitudes of the principal stresses in the imposed stress state, therefore a robust analysis can be performed without precise knowledge of stress magnitudes.

### 4.3 Dilation tendency and slip tendency analysis

The three faults investigated here each show a diverse spectrum of dilation tendency and slip tendency associated with their orientation (primarily dip but also strike) changes (**Fig. 4**). Comparing the dilation tendency and slip tendency profiles shows segments that fall into 3 primary categories: (i) low dilation tendency and low slip tendency, (ii) moderately high dilation tendency and high slip tendency, and (iii) high dilation tendency and low slip tendency. Cross plotting dilation tendency versus slip tendency for measured fault orientations (strike and dip measurements) shows this diverse spectrum of resolved stress characteristics (**Fig. 5**). Differentiating between observations of calcite vein cement versus slickenlines associated with these fault segments shows a clear pattern of calcite vein cement associated with fault segments that have high dilation tendency and low to moderately high slip tendency ( $\times$  symbol in **Fig. 5**). Slickenlines were observed on fault segments that have moderately high to low dilation tendency and high to moderately low slip tendency ( $+$  symbol in **Fig. 5**). Depth intervals for measurement locations on the analysed faults are as follows: (i) Textbook fault = 0.05 to 0.6 m, (ii) Spanish Goat fault = 0.05 m to 0.4 m, (iii) Big Indigo fault = 0.05 to 0.45 m. Systematic sampling more coarsely than this would underrepresent the fault irregularity and refraction that produced the dilation and localized fluid flow along the faults.

The moderate to high slip tendency and high dilation tendency of the steepest segments (dips  $>75^\circ$ , red points) is consistent with hybrid failure. High slip tendency and moderately high dilation tendency for moderate to steep fault segments (dips of  $45^\circ$ - $75^\circ$ , green and gold points) is consistent with shear failure, whereas the moderate to low slip tendency and low dilation tendency of the most gently dipping segments (dips  $<45^\circ$ , light blue and dark blue points) is more consistent with compactive shear failure, although no definitive evidence of compactive shear (e.g., slickolites) was observed in the field (see **Fig. 1** for comparison). The pattern of dilation tendency versus slip tendency on the fault segments matches well with the deformation processes indicated by vein material indicative of dilation versus absence of vein material and presence of slickenlines indicative of sliding (**Fig. 5**).

Fault refraction through the mechanically layered Eagle Ford lithostratigraphic section led to conduit development at dilational segments along faults (**Fig. 6a**). These conduits are structurally controlled and form along the fault/bedding intersection within more competent (chalk) beds where steep fault segments experienced dilation (dilational jogs; Ferrill and Morris, 2003; Ferrill et al. 2014a). Conduits tend to parallel the intermediate principal stress direction, which is horizontal or nearly horizontal in normal and thrust faulting stress regimes (e.g., Ferrill et al., 2019a, 2020), and vertical in a strike slip regime (Giorgetti et al., 2016; Carlini et al., 2019).

For a cohesionless fault, slip tendency at the initiation of slip is expected to equal the coefficient of friction on the fault (e.g., Byerlee, 1978; Morris et al., 1996). A fault that has slip tendency equal to the coefficient of friction is considered “critically stressed” (Stock et al., 1985; Barton et al., 1995; Morris et al., 1996; Zoback et al., 1996). This study shows that the slip tendency was highly variable along the refracted faults at the time of their active slip. Slip tendencies (**Fig. 5**) ranged from high values ( $>0.6$ ), consistent with coefficients of friction of 0.6 to 0.85 described by Byerlee (1978), to low or very low values (0.4 to  $<0.2$ ) on gently dipping fault segments that would make sense for activity only for low coefficients of friction associated with weak rock (see coefficient of friction summary in Ferrill et al., 2017b). Different rock types inherently have different friction coefficients, so a mechanical multilayer like the Eagle Ford Formation that includes chalk, marl, mudrock, and volcanic ash should be expected to have variable slip tendencies required to overcome the variable friction coefficients through different mechanical layers (**Fig. 6b**). Because of the different mechanical properties of mudrock and chalk, lead to different responses to loading conditions and produces significantly different pre-failure responses in mudrock versus chalk, and therefore different effective stress conditions from one mechanical layer to the next through the section. We are not specifically interpreting whether mudrock or chalk failed first. However, the repeated occurrence of refracted fault propagation through the section, contrasting mechanical properties of chalk and mudrock, and absence of widespread hybrid failure in chalk beds or shear failure in mudrock that is unassociated with larger multi-bed faults, suggests distinctly different effective stress conditions in mudrock and chalk shown in Fig. 6b likely coexisted in adjacent beds during fault propagation.

385 The clear relationships displayed in the dilation tendency versus slip tendency pattern, the failure and reactivation modes, and the mechanical layering, demonstrates the importance of understanding this interplay when investigating fault-related permeability development. Unconventional hydrocarbon reservoirs and low-permeability seal strata for aquifers, oil and gas reservoirs, and CO<sub>2</sub> reservoirs or sequestration sites are commonly not lithologically homogeneous, but instead are heterolithic and mechanically layered (e.g., [Alves and Elliot, 2014](#); [Petrie et al., 2014](#); [Ward et al., 2016](#); [Roelofse et al., 2019](#); [Mioicic et al., 2020](#)). Consequently, failure modes and failure orientations are likely to vary bed to bed and result in refracted fault shapes and fluid pathways similar to those discussed here.

390 The analysis in this paper clearly shows that deformation behaviour is intimately related to the orientation of the deformation feature with respect to the stress field in which it is active. Important orientation changes along the faults investigated here occur on the scale of individual beds over distances of cm's to 10's of cm. Generalized or smoothed fault shapes would not be representative of the actual behaviour of the fault. It is worth noting that fault refraction also occurs at much larger scales related to mechanical stratigraphy (see discussion in [Ferrill et al., 2017b](#)). To capture the important the orientation variability that is critical to dilation tendency and slip tendency analysis requires careful mapping of the orientation changes in the maximum detail possible. Ze and Alves (2019) evaluated the influence of sampling on displacement characterization and segment identification for faults mapped with 3D seismic reflection data and concluded that a sampling interval on the scale of 3% to 5% of fault length was needed for robust analysis. As detailed mapping and close sample spacing is critical to identifying displacement changes and segments along faults (e.g., [Wyrick et al., 2011](#); [Ze and Alves, 2019](#)), it is also critical to predicting the deformation behaviour using dilation tendency and slip tendency analysis.

395  
400

The actual fault orientation variability described in the present study, however, is far too fine-scale to be mapped with seismic reflection data. Although the overall shape of a normal fault through the Eagle Ford Formation or similar rock that has throw of >10-20 m may be mappable from 3D seismic data, the bed-scale orientation variability along it will not be mappable. Using detailed mechanical stratigraphic characterization (e.g., from microrebound analysis of core), stress inversion, and understanding gained from this and other detailed investigations, failure mode prediction can help to bridge this gap and inform realistic representation of fault zone complexity.

405

## 6 Conclusions

410 Faults investigated here were active with refracted dip profiles with segments that experienced widely varying dilation tendencies and slip tendencies at the time of activity. Deformation modes correlate with the dilation and slip tendency changes, and show that neither slip tendency nor dilation tendency alone are complete indicators of fault zone behaviour. The integrated analysis of dilation tendency and slip tendency, however, can be a very effective means to predict deformation behaviour for fault segments or other structural features (fractures, layer boundaries, or mechanical interfaces). This deformation behaviour is intimately related to the orientation of the deformation feature with respect to the stress field in which it is active, occurring on the scale of individual lithologic beds over distances of cm's to 10's of cm. To capture the important ~~the~~ orientation variability that is critical to dilation tendency and slip tendency analysis requires careful mapping of the orientation changes in the maximum detail possible, and may require failure mode prediction based on detailed mechanical stratigraphic, stress, and geomechanical analysis informed by results of this and other detailed studies.

415

420

*Acknowledgements.* Slip and dilation tendency analyses were performed using 3DStress® v. 5.1. We thank Janice Moody and Heath Grigg for allowing us research access to the Rancho Rio Grande. Financial support for this work was provided by Southwest Research Institute's Eagle Ford joint industry project, funded by Anadarko Petroleum Corporation, BHP Billiton, Chesapeake Energy Corporation, ConocoPhillips, Eagle Ford TX LP, EP Energy, Hess Corporation, Marathon Oil Corporation, Murphy Exploration and Production Company, Newfield Exploration Company, Pioneer Natural Resources, and Shell. We thank the staff of these sponsor companies for the interaction and constructive feedback. Analyses in this manuscript were also supported in part by SwRI® Internal Research and Development Project R8940. We thank Ronald McGinnis, Dan Lehrmann, Erich DeZoeten, Sarah Wigginton, and Zach Sickmann for their contributions to data collection. Constructive comments by Tiago Alves and Fabio Trippetta greatly improved the final version of this paper.

425

430 **References**

- Alves, T. A. and Elliott, C.: Fluid flow during early compartmentalisation of rafts: A North Sea analogue for divergent continental margins. *Tectonophysics*, 634, 91-96, <http://dx.doi.org/10.1016/j.tecto.2014.07.015>, 2014.
- Anderson, E. M.: The dynamics of faulting and dyke formation with applications to Britain. Oliver and Boyd, Edinburgh, 1951.
- 435 Barton, C. A., Zoback, M. D., and Moos, D.: Fluid flow along potentially active faults in crystalline rock. *Geology*, 23, 683–686, 1995.
- Bodziak, R., Clemons, K., Stephens, A., and Meek, R.: The role of seismic attributes in understanding the ‘frac-able’ limits and reservoir performance in shale reservoirs: An Example from the Eagle Ford Shale, South Texas, USA, *Am. Assoc. Pet. Geol. Bull.*, 98, 2217–2235, 2014.
- 440 Boersma, Q. D., Douma, L. A. N. R., Bertotti, G., and Barnhoorn, A.: Mechanical controls on horizontal stresses and fracture behaviour in layered rocks: A numerical sensitivity analysis. *J. Struct. Geol.*, 130, <https://doi.org/10.1016/j.jsg.2019.103907>, 2020.
- Breyer, J. A.: The Eagle Ford Shale: a Renaissance in U.S. Oil Production: American Association of Petroleum Geologists, Memoir 110, 399 p. 2016.
- 445 Buseti, S., Jiao, W., and Reches, Z.: Geomechanics of hydraulic fracturing microseismicity: Part 1. Shear, hybrid, and tensile events. *Am. Assoc. Pet. Geol. Bull.*, 98, 2439–2457, 2014.
- Byerlee, J.: Friction of rocks. *Pure and Applied Geophysics*, 116, 615–626, 1978.
- Caine, J. S., Evans, J. P., and Forster, C. B.: Fault zone architecture and permeability structure, *Geology*, 24, 1025–1028, 1996.
- 450 Carlini, M., Viola, G., Mattila, J., and Castellucci, L.: The role of mechanical stratigraphy on the refraction of strike-slip faults, *Solid Earth*, 10, 343–356, <https://doi.org/10.5194/se-10-343-2019>, 2019.
- Carlsson, A. and Olsson, T.: Hydraulic conductivity and its stress dependence. *Proceedings, Paris, Workshop on Low-Flow, Low-Permeability Measurements in Largely Impermeable Rocks*, 249–259, 1979.

- Cusack, C., Beeson, J., Stoneburner, D., and Robertson, G.: The discovery, reservoir attributes, and significance of the  
455 Hawkville Field and Eagle Ford Shale trend, Texas, Gulf Coast Association of Geological Societies Transactions, 60,  
165–179, 2010.
- Denney, D.: Improve unconventional reservoir completion and stimulation effectiveness. J. Petrol. Technol., 64(10),  
<http://dx.doi.org/10.2118/1012-0115-JPT>, 2012.
- Douma, L. A. N. R., Regelink, J. A., Bertotti, G., Boersma, Q. D., and Barnhoorn, A.: The mechanical contrast between layers  
460 controls fracture containment in layered rocks, J. Struct. Geol., 127, <https://doi.org/10.1016/j.jsg.2019.06.015>, 2019.
- Edman, J. D. and Pitman, J. K.: Geochemistry of Eagle Ford Group source rocks and oils from the First Shot Field area, Texas,  
Trans. GCAGS 60, 217–234, 2010.
- Evans, J. P., Forster, C. B., and Goddard, J. V.: Permeability of fault-related rocks, and implications for hydraulic structure of  
fault zones. J. Struct. Geol., 19, 1393–1404, 1997.
- 465 Faulkner, D. R., Jackson, C. A. L., Lunn, R. J., Schlische, R. W., Shipton, Z. K., Wibberley, C. A. J., and Withjack, M. O.: A  
review of recent developments concerning the structure, mechanics and fluid flow properties of fault zones. J. Struct.  
Geol., 32, 1557–1575, 2010.
- Ferrill, D. A. and Morris, A. P.: Dilational normal faults, J. Struct. Geol., 25, 183–196, [https://doi.org/10.1016/S0191-  
8141\(02\)00196-7](https://doi.org/10.1016/S0191-8141(02)00196-7), 2003.
- 470 Ferrill, D. A., Winterle, J., Wittmeyer, G., Sims, D., Colton, S., Armstrong, A., and Morris, A. P.: Stressed rock strains  
groundwater at Yucca Mountain, Nevada, GSA Today, 9, 1–8, 1999.
- Ferrill, D. A., Sims, D. W., Waiting, D. J., Morris, A. P., Franklin, N., Schultz, A. L.: Structural Framework of the Edwards  
Aquifer recharge zone in south-central Texas, Geol. Soc. Am. Bull. 116, 407–418, 2004.
- Ferrill, D. A., McGinnis, R. N., Morris, A. P., and Smart, K. J.: Hybrid failure: Field evidence and influence on fault refraction,  
475 J. Struct. Geol., 42, 140–150, <https://doi.org/10.1016/j.jsg.2012.05.012>, 2012.
- Ferrill, D. A., McGinnis, R. N., Morris, A. P., Smart, K. J., Sickmann, Z. T., Bentz, M., Lehrmann, D., and Evans, M. A.:  
Control of mechanical stratigraphy on bed-restricted jointing and normal faulting: Eagle Ford Formation, south-central  
Texas, U.S.A., Am. Assoc. Pet. Geol. Bull., 98, 2477–2506, 2014a.

- Ferrill, D. A., Morris, A. P., Hennings, P. H., and Haddad, D. E.: Faulting and fracturing in shale and self-sourced reservoirs: Introduction, *Am. Assoc. Pet. Geol. Bull.*, 98, 2161–2164, 2014b.
- Ferrill, D. A., Evans, M. A., McGinnis, R. N., Morris, A. P., Smart, K. J., Wigginton, S. S., Gulliver, K. D. H., Lehrmann, D., de Zoeten, E., and Sickmann, Z.: Fault zone processes in mechanically layered mudrock and chalk, *J. Struct. Geol.*, 97, 118–143, 2017a.
- Ferrill, D. A., Morris, A. P., McGinnis, R. N., Smart, K. J., Wigginton, S. S., and Hill, N. J.: Mechanical stratigraphy and normal faulting, *J. Struct. Geol.*, 94, 275–302, <https://doi.org/10.1016/j.jsg.2016.11.010>, 2017b.
- Ferrill, D. A., Smart, K. J., and Morris, A. P.: Fault failure modes, deformation mechanisms, dilation tendency, slip tendency, and conduits v. seals. in: *Integrated Fault Seal Analysis*, edited by: Ogilvie, S. R., Dee, S. J., Wilson, R. W. & Bailey, W. R., Geological Society, London, Special Publications, 496, <https://doi.org/10.1144/SP496-2019-7>, 2019a.
- Ferrill, D. A., Morris, A. P., and McGinnis, R. N.: Geologic structure of the Edwards (Balcones Fault Zone) Aquifer, in Sharp, J.M., Jr., Green, R.T., and Schindel, G.M., eds., *The Edwards Aquifer: The Past, Present, and Future of a Vital Water Resource: Geological Society of America Memoir 215*, 171–188, [https://doi.org/10.1130/2019.1215\(14\)](https://doi.org/10.1130/2019.1215(14)), 2019b.
- Ferrill, D. A., Evans, M. A., McGinnis, R. N., Morris, A. P., Smart, K. J., Lehrmann, D., Gulliver, K. D. H., and Sickmann, Z.: Fault zone processes and fluid history in Austin Chalk, southwest Texas, *Am. Assoc. Pet. Geol. Bull.*, 104 (2), 245–283, <https://doi.org/10.1306/04241918168>, 2020.
- Gale, J. F. W., Laubach, S. E., Olson, J. E., Eichhubl, P., and Fall, A.: Natural fractures in shale: a review, *Am. Assoc. Pet. Geol. Bull.*, 98, 2165–2216, 2014.
- Giorgetti, C., Collettini, C., Scuderi, M. M., and Tesei, T.: Fault geometry and mechanics of marly carbonate multilayers: An integrated field and laboratory study from the Northern Apennines, Italy, *J. Struct. Geol.*, 93, 1–16, 2016.
- Hancock, P. L.: Brittle microtectonics: principles and practice, *J. Struct. Geol.*, 7, 437–457, 1985.
- Kornacki, A. S.: Production of migrated oil from the Eagle Ford source-rock reservoir at a moderate level of thermal maturity: Unconventional Resources Technology Conference (URTeC), DOI 10.15530/urtec-2018-2871569, 16 p., 2018.
- Lee, Y.-J. and Wiltschko, D. V.: ~~2000~~, Fault controlled sequential vein dilation: competition between slip precipitation rates in the Austin Chalk, Texas, *J. Struct. Geol.*, 22, 1247–1260, [2000](https://doi.org/10.1016/0197-5707(00)00050-9).

- Lee, Y.-J., Wiltschko, D. V., Grossman, E. L., Morse, J. W., and Lamb, W. M.: Sequential vein growth with fault displacement: An example from the Austin Chalk Formation, Texas, *J. Geophys. Res.*, 102, 22,611–22,628, 1997.
- Lehrmann, D. J., Yang, W., Sickmann, Z.T., Ferrill, D. A., McGinnis, R. N., Morris, A. P., Smart, K. J., Gulliver, K. D. H.: Controls on sedimentation and cyclicity of the Eagle Ford and Lower Austin Chalk (and equivalent Boquillas Formation) from detailed outcrop studies of western and central Texas. *Journal of Sedimentary Research*, v. 89, 629–653, DOI: <http://dx.doi.org/10.2110/jsr.2019.38>, 2019.
- 510 Livingston, P., Sayre, A. N., White, W. N.: Water Resources of the Edwards Limestone in the San Antonio Area, Texas, United States Department of the Interior, Water-Supply Paper 773-B, 59–113, 1936.
- Maclay, R. W.: Edwards Aquifer in San Antonio: Its hydrogeology and management, *Bulletin of the South Texas Geological Society*, 30(4), 11–28, 1989.
- Maclay, R. W. and Small, T. A.: Hydrostratigraphic subdivisions and fault barriers of the Edwards Aquifer, south-central Texas, USA, *Journal of Hydrology*, 61, 127–146, 1983.
- 515 Maher, H. D.: Distributed normal faults in the Niobrara Chalk and Pierre Shale of the central Great Plains of the United States, *Lithosphere*, 6, 319–334, 2014.
- Martin, R., Baihly, J., Malpani, R., Lindsay, G., and Atwood, L.: Understanding production from Eagle Ford-Austin Chalk system. In: Society of Petroleum Engineers Annual Technical Conference and Exhibition, 30 October e 2 November. Society of Petroleum Engineers, Denver, Colorado, 2011.
- 520 Mattos, N. H. and Alves, T. M.: Corridors of crestal and radial faults linking salt diapirs in the Espírito Santo Basin, SE Brazil. *Tectonophysics*, 728-729, 55–74, <https://doi.org/10.1016/j.tecto.2017.12.025>, 2018.
- Mattos, N. H., Alves, T. M., Omosanya, K. O.: Crestal fault geometries reveal late halokinesis and collapse of the Samson Dome, Northern Norway: Implications for petroleum systems in the Barents Sea. *Tectonophysics*, 690, 76–96, <http://dx.doi.org/10.1016/j.tecto.2016.04.043>, 2016.
- 525 McFarland, J., Morris, A. P., and Ferrill, D. A.: Stress inversion using slip tendency, *Computers and Geosciences*, 41, 40–46, 2012.

- 530 Meng, J., Pashin, J., Chandra, A., Xue, L., Sholanke, S., and Spears, J.: Structural framework and fault analysis in the east-central Gulf of Mexico shelf: Implications for offshore CO<sub>2</sub> storage. J. Struct. Geol., 134, <https://doi.org/10.1016/j.jsg.2020.104020>, 2020.
- Miocic, J. M., Johnson, G., and Gilfillan, S. M. V.: Stress field orientation controls fault leakage at a natural CO<sub>2</sub> reservoir, Solid Earth, <https://doi.org/10.5194/se-2020-12>, 2020.
- Morris, A. P., Ferrill, D. A., and Henderson, D. B.: Slip tendency analysis and fault reactivation, Geology, 24, 275–278, 1996.
- Morris, A. P., Ferrill, D. A., and McGinnis, R. N.: Using fault displacement and slip tendency to estimate stress states. J. Struct. Geol., 83, 60–72, 2016.
- 535 Petrie, E. S., Evans, J. P., and Bauer, S. J.: Failure of cap-rock seals as determined from mechanical stratigraphy, stress history, and tensile-failure analysis of exhumed analogs. Am. Assoc. Pet. Geol. Bull., 98, 2365–2389, 2014.
- Ramsey, J. M. and Chester, F. M.: Hybrid fracture and the transition from extension fracture to shear fracture. Nature, 428, 63–66, 2004.
- 540 Roelofse, C., Alves, T. M., Gafeira, J., and Omosanya, K. O.: An integrated geological and GIS-based method to assess caprock risk in mature basins proposed for carbon capture and storage. International Journal of Greenhouse Gas Control, 80, 103–122, <https://doi.org/10.1016/j.ijggc.2018.11.007>, 2019.
- Roelofse, C., Alves, T. M., and Gafeira, J.: Structural controls on shallow fluid flow and associated pockmark fields in the East Breaks area, northern Gulf of Mexico. Marine and Petroleum Geology, 112, <https://doi.org/10.1016/j.marpetgeo.2019.104074>, 2020.
- 545 Robinson, C.R., 1997. Hydrocarbon source rock variability within the Austin Chalk and Eagle Ford Shale (Upper Cretaceous), East Texas, U.S.A. Int. J. Coal Geol. 34, 287–305.
- Schöpfer, M. P. J., Childs, C., and Walsh, J. J.: Localization of normal faults in multilayer sequences. J. Struct. Geol., 28, 816–833, 2006.
- 550 Sibson, R. H.: Structural permeability of fluid-driven fault-fracture meshes, J. Struct. Geol., 18, 1031–1042, [https://doi.org/10.1016/0191-8141\(96\)00032-6](https://doi.org/10.1016/0191-8141(96)00032-6), 1996.

- Sibson, R. H.: Brittle failure mode plots for compressional and extensional tectonic regimes, *J. Struct. Geol.*, 20, 655–660, [https://doi.org/10.1016/S0191-8141\(98\)00116-3](https://doi.org/10.1016/S0191-8141(98)00116-3), 1998.
- 555 Sibson, R. H.: Fluid involvement in normal faulting, *J. Geodyn.*, 29, 469–499, [https://doi.org/10.1016/S0264-3707\(99\)00042-3](https://doi.org/10.1016/S0264-3707(99)00042-3), 2000.
- Sibson, R. H.: Brittle-failure controls on maximum sustainable overpressure in different tectonic regimes, *Am. Assoc. Pet. Geol. Bull.*, 87, 901–908, <https://doi.org/10.1306/01290300181>, 2003.
- Sibson, R. H. and Scott, J.: Stress/fault controls on the containment and release of overpressured fluids: examples from gold-quartz vein systems in Juneau, Alaska; Victoria, Australia and Otago, New Zealand, *Ore Geol. Rev.*, 13, 293–306, [https://doi.org/10.1016/S0169-1368\(97\)00023-1](https://doi.org/10.1016/S0169-1368(97)00023-1), 1998.
- 560
- Smart, K. J., Ofoegbu, G. I., Morris, A. P., McGinnis, R. N., and Ferrill, D. A.: Geomechanical modeling of hydraulic fracturing: Why mechanical stratigraphy, stress state, and pre-existing structure matter. *Am. Assoc. Pet. Geol. Bull.*, 98, 2237–2261, 2014.
- Stock, J. M., Healy, J. H., Hickman, S. H., and Zoback, M. D.: Hydraulic fracturing stress measurements at Yucca Mountain, Nevada, and relationship to regional stress field, *J. Geophys. Res.*, 90, 8691–8706, 1985.
- 565
- Thompson, R. C.: Post-Laramide, collapse-related fracturing and associated production; Wind River Basin, Wyoming, *The Mountain Geologist*, 52(4), 27–46, 2015.
- Trippetta, F., Collettini, C., Barchi, M. R., Lupattelli, A., and Mirabella, F.: A multidisciplinary study of a natural example of a CO<sub>2</sub> geological reservoir in central Italy. *International Journal of Greenhouse Gas Control*, 12, 72–83, <https://doi.org/10.1016/j.ijggc.2012.11.010>, 2013.
- 570
- Trippetta, F., Carpenter, B. M., Mollo, S., Scuderi, M. M., Scarlato, P., and Collettini, C.: Physical and transport property variations within carbonate-bearing fault zones: Insights from the Monte Maggio fault (central Italy). *Geochemistry, Geophysics, Geosystems*, 18(11), 4027–4042, <https://doi.org/10.1002/2017GC007097>, 2017.
- Ward, N. I. P., Alves, T. M., Blenkinsop, T. G.: Reservoir leakage along concentric faults in the Southern North Sea: Implications for the deployment of CCS and EOR techniques. *Tectonophysics*, 690, 97–116, <http://dx.doi.org/10.1016/j.tecto.2016.07.027>, 2016.
- 575

Wyrick, D. Y., Morris, A. P., Ferrill, D. A.: [Normal fault growth in analog models and on Mars. Icarus, doi:10.1016/j.icarus.2011.01.011, 2011.](https://doi.org/10.1016/j.icarus.2011.01.011)

580

[Ze, T. and Alves, T. M.: The role of gravitational collapse in controlling the evolution of cretal fault systems \(Espírito Santo Basin, SE Brazil\). Journal of Structural Geology, 92, 79–98, http://dx.doi.org/10.1016/j.jsg.2016.09.011, 2016.](https://doi.org/10.1016/j.jsg.2016.09.011)

[Ze, T. and Alves, T. M.: The role of gravitational collapse in controlling the evolution of cretal fault systems \(Espírito Santo Basin, SE Brazil\) – Reply. Journal of Structural Geology, 98, 12–14, http://dx.doi.org/10.1016/j.jsg.2017.03.005, 2017.](https://doi.org/10.1016/j.jsg.2017.03.005)

[Ze, T. and Alves, T. M.: Impacts of data sampling on the interpretation of normal fault propagation and segment linkage. Tectonophysics, 762, 79–96, https://doi.org/10.1016/j.tecto.2019.03.013, 2019.](https://doi.org/10.1016/j.tecto.2019.03.013)

585

Zoback, M., Barton, C., Finkbeiner, T., and Dholakia, S.: Evidence for fluid flow along critically-stressed faults in crystalline and sedimentary rock. In: Jones, G., Fisher, Q., Knipe, R. (Eds.), *Faulting, Faults Sealing and Fluid Flow in Hydrocarbon Reservoirs*, 47–48, University of Leeds, England, 1996.

Zumberge, J., Illisch, H., and Waite, L.: Petroleum geochemistry of the Cenomanian-Turonian Eagle Ford oils of south Texas, AAPG Memoir 110, 135–165, 2016.

590

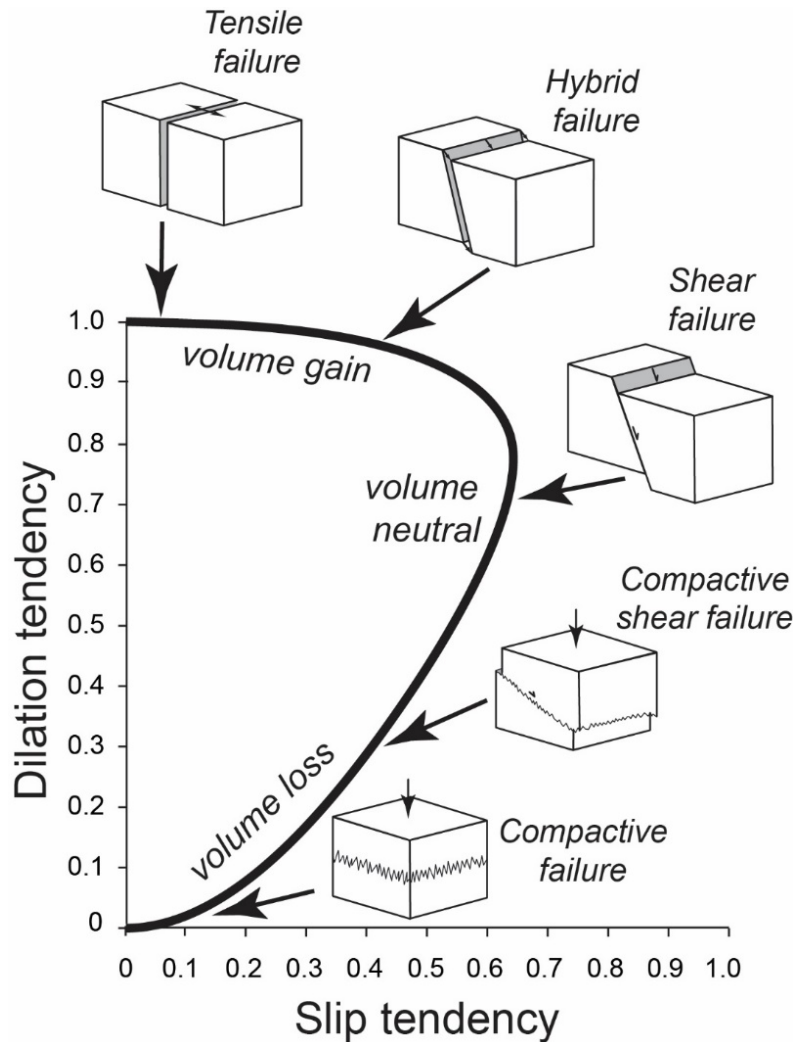


**Figure 1.** General graphical relationship between maximum slip tendency and dilation tendency, and associated rock failure modes and volume change (from Ferrill et al., 2019a). As discussed by Ferrill et al. (2019a), analysing faults in this parameter space shows promise for prediction of the failure or deformation modes and the associated conduit versus seal behaviour. For purposes of this illustration, representative deformation features are shown for a normal faulting stress regime.

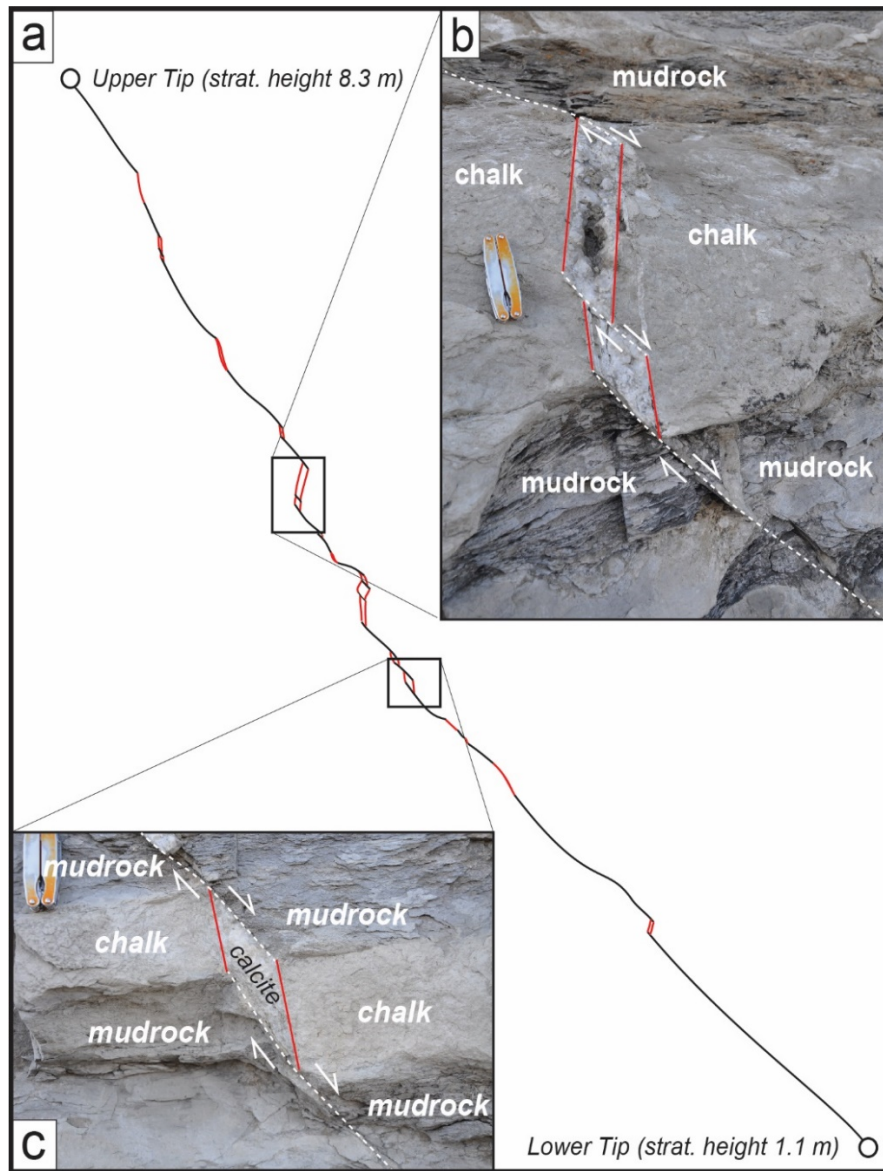
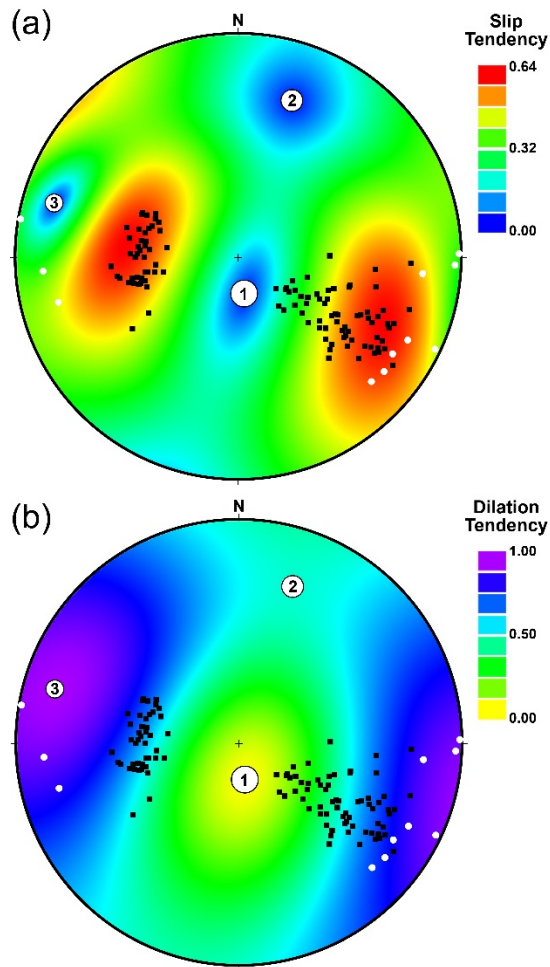


**Figure 2.** Details of the Textbook fault in Eagle Ford Formation outcrop at Sycamore Bluffs in southwest Texas. See Ferrill et al. (2017a) for additional detail on the exposure and faults. The section is heterolithic, including primarily chalk, marl, and calcareous mudrock. Faults tend to be represented by shear failure through mudrock, and hybrid failure through chalk beds, resulting in refracted fault profiles that exhibit dilation of steep segments through chalk beds. Dilation segments are represented by mechanical aperture that is partially cemented with calcite (see part **b**) or completely cemented with calcite (see part **c**).



605

**Figure 3.** Equal-angle stereonet plots of (a) slip tendency and (b) dilation tendency (bottom) with poles to shear segments (black dots) and calcite cemented dilational segments (white dots) measured from the Textbook, Spanish Goat, and Big Indigo faults at Sycamore Bluffs. Larger dots labelled 1, 2, and 3 represent orientations of the maximum, intermediate, and minimum principal compressive stresses,  $\sigma_1$ ,  $\sigma_2$ , and  $\sigma_3$ , respectively. See text for further discussion of the inferred stress tensor.

610

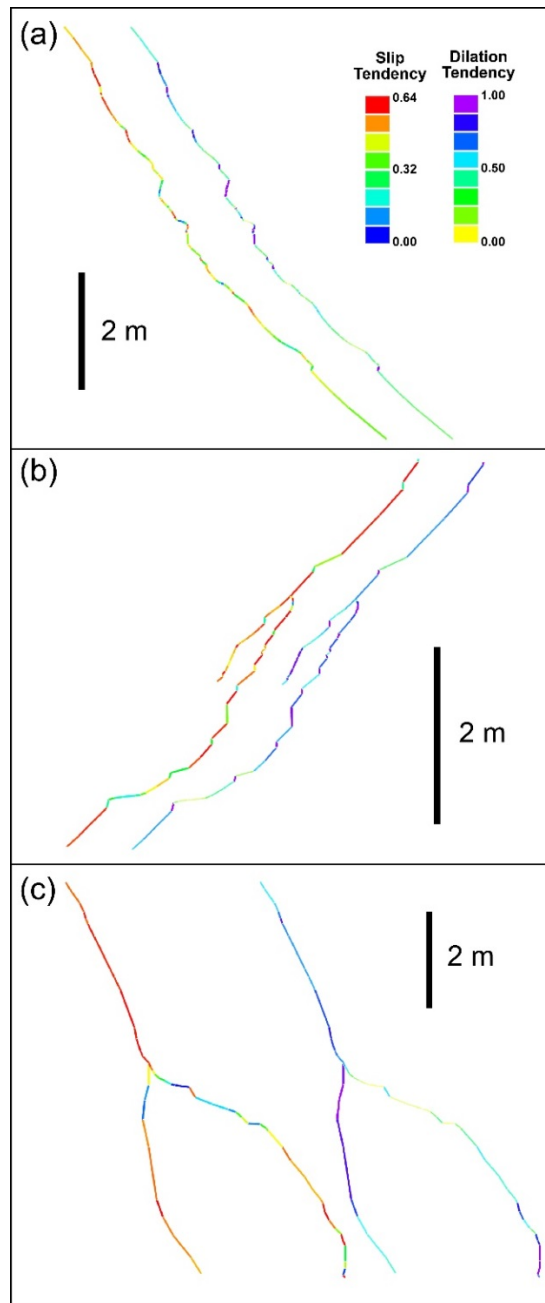


**Figure 4.** Slip tendency (left profile of each pair) and dilation tendency (right profile of each pair) profiles of the (a) Textbook, (b) Spanish Goat, and (c) Big Indigo faults at Sycamore Bluffs using the inverted stress tensor described in the text and 615 illustrated in terms of slip tendency and dilation tendency in **Fig. 3**. Although these plots are similar to those presented in Ferrill et al. (2017a), they have been updated to reflect the inverted stress state shown in **Fig. 3**.

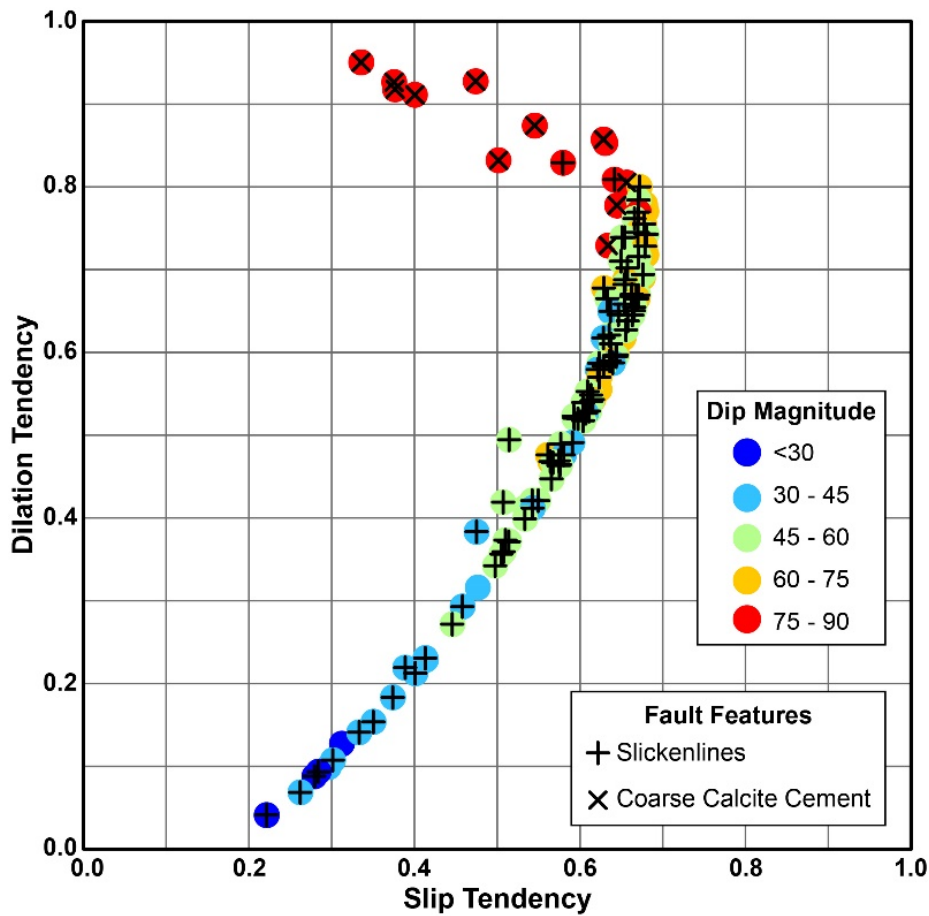


**Figure 5.** Comparison of dilation tendency and slip tendency for measured fault segments of the Textbook, Spanish Goat, and Big Indigo faults, color-coded by dip, with + and × symbols indicating presence of slickenlines or coarse calcite cement, respectively. The few colored dots that lack additional symbols exhibit shear displacements either lack slickenlines, or slickenlines could not be seen due to the planar outcrop surface in some locations. The moderate to high slip tendency and high dilation tendency of the steep segments (dips  $>75^\circ$ , red points) are consistent with hybrid failure, whereas the moderate to low slip tendency and low dilation tendency of the most gently dipping segments (dips  $<45^\circ$ , light blue and dark blue points) are suggestive of compactive shear. See **Fig. 1** for comparison.

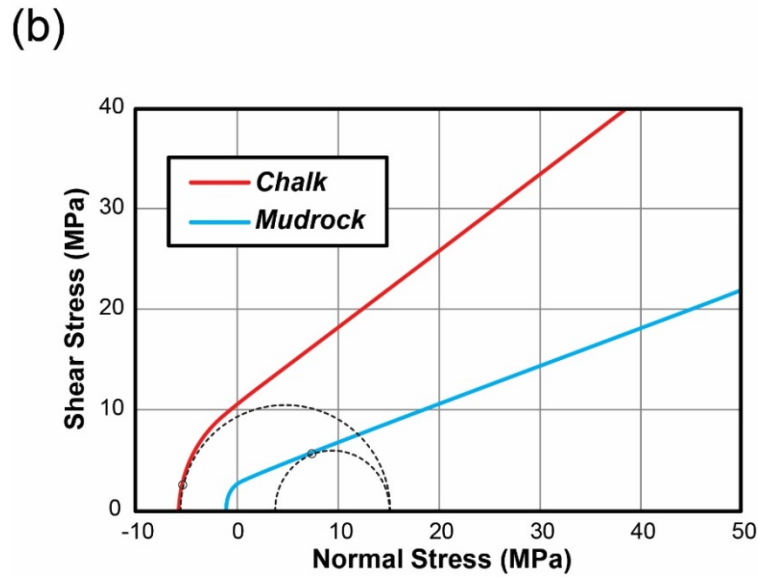
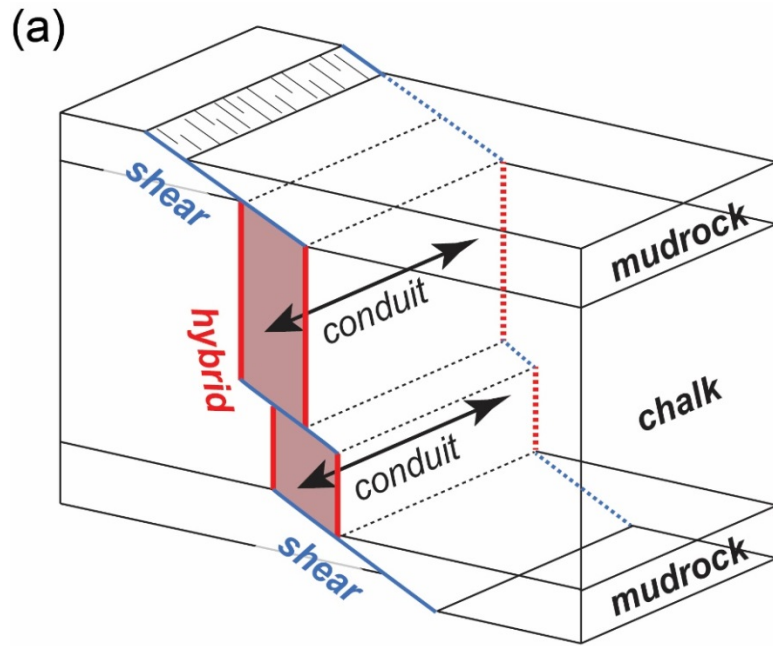


**Figure 6.** (a) Schematic block diagram illustrating the change in failure angle and mode from mudrock to chalk, and the associated dilation of the steeper hybrid segment and formation of a fault conduit parallel to the fault-bedding intersection direction. (b) Interpreted failure envelopes and stress circles for chalk and mudrock at the time of failure with a uniform effective overburden stress of 20-15 MPa (corrected for pore fluid pressure) with hybrid failure predicted for the more competent chalk beds and shear failure predicted for the less competent mudrock.